Improving the Total Impulse Capability of the NSTAR Ion Thruster with Thick-Accelerator-Grid Ion Optics*†

George C. Soulas
NASA Glenn Research Center
M.S. 301-3
21000 Brookpark Road
Cleveland, OH 44135, U.S.A.
216-977-7419
George.C.Soulas@grc.nasa.gov

IEPC-01-081

The results of performance tests with thick-accelerator-grid (TAG) ion optics are presented. TAG ion optics utilize a 50% thicker accelerator grid to double ion optics' service life. NSTAR ion optics were also tested to provide a baseline performance for comparison. Impingement-limited total voltages for the TAG ion optics were only 0-15 V higher than those of the NSTAR ion optics. Electron backstreaming limits for the TAG ion optics were 3-9 V higher than those for the NSTAR optics due to the increased accelerator grid thickness for the TAG ion optics. Screen grid ion transparencies for the TAG ion optics were only about 2% lower than those for the NSTAR optics, reflecting the lower physical screen grid open area fraction of the TAG ion optics. Accelerator currents for the TAG ion optics were 19-43% greater than those for the NSTAR ion optics due, in part, to a sudden increase in accelerator current during TAG ion optics' performance tests for unknown reasons and to the lower-than-nominal accelerator aperture diameters. Beam divergence half-angles that enclosed 95% of the total beam current and beam divergence thrust correction factors for the TAG ion optics were within 2º and 1%, respectively, of those for the NSTAR ion optics.

Introduction

The success of the NSTAR (i.e. NASA Solar Electric Propulsion Technology Applications Readiness Program) 30 cm ion thruster system on the Deep Space 1 mission has demonstrated the viability of ion propulsion for deep space missions.[1,2] As a result, ion propulsion is a candidate for several deep space missions, such as the Neptune Orbiter, Titan Explorer, Mars Sample Return, Europa Lander, and others. However, most of these missions require increasing the NSTAR thruster's propellant throughput and peak input power capabilities beyond the demonstrated 88 kg of xenon at 2.3 kW and approximately 140 kg at various power levels.[3-5]

The total impulse capability of the NSTAR ion thruster is limited, in part, by sputter erosion of the ion optics. Brophy, Polk, and Rawlin identified five credible failure modes related to sputter erosion of the NSTAR ion optics that must be addressed to increase optics longevity.[6] These failure modes included:

1. accelerator grid structural failure from charge-exchange ion sputter erosion of the downstream accelerator surface;
2. electron backstreaming due to enlargement of the accelerator grid apertures from charge-exchange ion sputter erosion;
3. a grid electrical short that cannot be eliminated by the grid clearing circuit;
4. screen grid sputter erosion by discharge chamber ions; and

* Presented as Paper IEPC-01-081 at the 27th International Electric Propulsion Conference, Pasadena, CA, 15-19 October, 2001.

5. accelerator grid structural failure due to direct ion impingement from defocused beamlets as a result of foreign material on a screen grid aperture.

The foreign material of failure mode 5 is generally presumed to originate either from the discharge chamber walls or cathode assembly as sputter-deposited material that had spalled or debris from a foreign source.[6] As a result, the discharge chamber flake containment design of the source of debris, and not the ion optics, controls failure mode 5. Although the downstream side of the NSTAR screen grid is sputter-deposited with accelerator grid material during operation,[3] spalling of this material would be expected to contribute to failure mode 3 (i.e. a grid electrical short) and not failure mode 5. Failure mode 5 will, therefore, not be considered here.

Test results from Ref. [3] also showed that screen grid sputter erosion (i.e. failure mode 4) was minimal, likely due to the derated operating conditions of the NSTAR thruster. Although screen grid erosion must be addressed in any ion optics' service life assessment, lifetimes well beyond those demonstrated in Refs. [3]-[5] are expected as long as these low discharge voltages and plasma densities are maintained and the ratio of doubly-to-singly charged ions is not significantly increased.

Long duration tests in the NSTAR program[3-5] and others[6,7] have demonstrated, however, that sputter erosion of the downstream surface and aperture walls of the accelerator grid (i.e. failure modes 1 and 2) must be addressed to increase ion optics' longevity. While accelerator aperture erosion would be expected to aggravate the issue of an unclearable electrical short (i.e. failure mode 3), grid shorting from accelerator grid erosion products was not found to be an issue during any long duration test of the NSTAR program.

A development effort to extend ion optics' service life was initiated at the NASA Glenn Research Center (GRC).[8] Several methods of extending ion optics' service life are presently being pursued. One method involves changing the ion optics' material to one with a lower volumetric sputter erosion rate than molybdenum. Grid material technologies presently investigated include carbon-based materials, titanium, and ion-implanted materials.[8-11]

Another method for increasing ion optics service life involves changing the ion optics' design and not the material. This prevents the loss of the large database already available with molybdenum ion optics and eliminates all fabrication development costs since the fabrication technique is unchanged. The ion optics' design change was to merely thicken the accelerator grid. Service life is enhanced primarily because there is more material available for sputter erosion. Additional benefits to thickening the accelerator grid include increased electron backstreaming limits and reduced neutral loss rates.

A service life assessment was conducted with thicker accelerator grids and compared to that of the NSTAR accelerator grid.[9] Service life analyses included, in part, sputter erosion of the downstream surface and aperture walls of the accelerator grid, shown in Fig. 1, and sputter erosion of the upstream surface of the screen grid. Failure criteria included accelerator grid structural failure from complete bridge erosion through the grid thickness, the onset of electron backstreaming from accelerator aperture enlargement, and screen grid structural failure from erosion through 50% of the grid thickness. Failure due to an unclearable grid electrical short was not assessed. The accelerator grid thickness for the thick-accelerator-grid (TAG) ion optics was increased 50% over the NSTAR accelerator grid thickness. This thickness was selected because the grid manufacturer had experience etching this thickness and there was prior performance test experience with this accelerator grid thickness.[12,13]

These analyses were conservative in that the accelerator voltage setting did not exploit the higher initial electron backstreaming limits of the TAG ion optics. Accelerator currents were, however, assumed to be the same as those of NSTAR ion optics. Results showed that TAG ion optics could more than double the NSTAR thruster total impulse capability at thruster input powers of 2.3 kW (i.e. the peak NSTAR input power), 3.0 kW, and 4.6 kW. The dominant failure mode was the onset of electron backstreaming from accelerator aperture enlargement at the grid center.

The following paper reports on the results of performance tests with TAG ion optics. These performance tests were conducted over a thruster input power range of 0.5 to 3.0 kW and are compared to those of NSTAR ion optics using the same thruster. Because prior tests with new titanium and

molybdenum ion optics had exhibited rapid initial changes in ion optics performance parameters, termed ion optics burn-in,[4,10,11] the TAG ion optics were initially operated until ion optics performance parameters achieved steady state values. Afterwards, ion optics' performance was determined. Ion optics performance parameters that included impingement-limited perveances, electron backstreaming limits, screen grid ion transparencies, accelerator currents, near-field beam current density profiles, beam divergence half-angles, and thrust correction factors due to beam divergence were determined throughout the thruster input power range.

Test Hardware and Operating Procedures

TAG Ion Optics

All nominal dimensions for the TAG ion optics were identical to the NSTAR design except for the accelerator grid thickness. The thickness for the TAG ion optics was increased 50% over the NSTAR thruster accelerator grid thickness. The nominal grid cold gap was set to the NSTAR dimension since prior testing had shown that this accelerator grid thickness had little effect on perveance.[13] Other electrode nominal dimensions were identical to those of the NSTAR thruster so that the NSTAR thruster ion optics mounting assembly design would require minimal changes.[14,15]

Two TAG ion optics sets were successfully manufactured. One TAG ion optics set was assembled for the tests reported here with hardware utilizing the NSTAR thruster design.[14] Screen and accelerator grid aperture diameter variations were within -1%/-5% and +0%/-22%, respectively, of the nominal NSTAR thruster design throughout the active area.[14,15] Screen and accelerator grid aperture diameters were smallest at the active area perimeter. The resulting screen and accelerator grid open area fractions at the active area perimeter were estimated to be about 9% and 30% lower-than-nominal, respectively. Grid cold gap variations throughout the active area were within +0%/-8% of the nominal NSTAR design. The center-to-center alignment of the screen and accelerator apertures was measured in the radial direction and found to be misaligned by as much as 10% of the nominal accelerator aperture diameter for the outer perimeter apertures. This misalignment was due to the increased thickness of the accelerator grid and was anticipated to cause the ion beam to be slightly more divergent.

NSTAR Ion Optics

NSTAR ion optics fabricated at NASA GRC were also tested to provide a baseline performance for comparison. Screen and accelerator grid aperture diameter variations were within +0%/–3% and ±4%, respectively, of the nominal NSTAR thruster design throughout the active area.[14,15] Accelerator grid aperture diameters were larger-than-nominal at the active area center while screen grid aperture diameters were lower-than-nominal at the active area perimeter. The resulting screen grid open area in the active area perimeter fraction was estimated to be only 3-4% lower-than-nominal. Grid cold gap variations throughout the active area were within ±8% of the nominal NSTAR thruster design.

Ion Thruster

Both ion optics sets were mounted onto a 30 cm ion thruster. This thruster serves as a test bed for 30 cm thruster development at NASA.[8] The mechanical designs of the thruster discharge chamber and ion optics were nearly identical to those of the NSTAR thruster, described in detail in Refs. [14] and [15]. The thruster was fitted with thermocouples for thermal tests and the exterior was modified so that a second neutralizer could be installed.

Power Console and Gas Feed System

A power console similar to that described in Ref. [16] powered the thruster. This power console was modified to allow the thruster to be throttled up to 5 kW. A high purity gas feed system was used to provide xenon to the discharge cathode, discharge chamber, and neutralizer through separate mass flow controllers.

Diagnostics

During thruster operation, voltages and currents were measured with digital multimeters and xenon flows with mass flow meters. These measured parameters were used to set thruster operating conditions, as well as to determine thruster performance.

The thruster was connected to an electrically floating power supply circuit used to determine the screen grid transparency to discharge chamber ions. The circuit electrically tied the screen grid to the discharge cathode during normal operation, but biased the grid

negative relative to discharge cathode potential to repel electrons and measure the collected ion current.[10,17]

Beam current density profiles were measured with a probe mounted onto a two-axis probe motion system. The probe was a planar geometry with a 1.0 cm^2 circular current-collecting area.[17] The probe was biased negative with respect to beam plasma potential to repel electrons and was grounded through a resistor that acted as a shunt to measure collected currents.

The positioning system swept the probe in the radial and axial directions through the vertical center of the thruster ion optics. The positioning system had a 1.25 m maximum travel in each axis, which enabled near-field radial beam current density measurements at different axial locations, as measured from the geometric center of the ion optics. The current density measurements were then used to determine beam current density profiles, beam divergence half-angles, and thrust correction factors.[10]

Vacuum Facility

Testing was conducted in Vacuum Facility 11 at NASA GRC. This 2.2 m diameter × 7.9 m long facility is evacuated with seven cryogenic pumps and a turbomolecular pump. The total measured facility pumping speed was greater than 100,000 l/s with xenon. The facility base pressure was typically less than 2.6×10^{-5} Pa and background pressures were as high as 5.2×10^{-4} Pa at the peak thruster input power of 3.0 kW.

Ion Optics Performance Parameters

Ion optics performance parameters were determined throughout testing. These parameters included impingement-limited total voltages, electron backstreaming limits, screen grid ion transparencies, accelerator grid currents, beam divergence, and beam divergence thrust losses.

Impingement-limited total voltages were determined from plots of accelerator current as a function of total voltage where the slope was -0.02 mA/V. Total voltage is the sum of the absolute values of the beam and accelerator power supply voltages. Perveance margins were defined as the difference between the total voltage during normal operation and the impingement-limited total voltage. Uncertainties in impingement-limited total voltage determinations (and, therefore, perveance margins) were within ±10 V.

The electron backstreaming limit was determined by lowering the magnitude of the accelerator grid voltage until the indicated beam current increased by 0.1 mA due to backstreaming electrons. Uncertainties in electron backstreaming limit measurements were estimated to be within ±1 V.

Screen grid ion transparencies were determined by biasing the screen grid 20 V below discharge cathode potential to repel electrons and to measure the collected ion current. The method used to determine screen grid ion transparency from these measurements is discussed in detail in Ref. [10]. Uncertainties in screen grid ion transparency measurements were estimated to be within ±0.002.

Radial beam current density profiles were used to determine beam divergence, and to provide peak current densities for comparisons of electron backstreaming limits.[10] Regarding beam current density measurements, no attempt was made to repel charge-exchange ions from the probe or to account for secondary electron emission due to ion bombardment. Integration of the radial beam current density profiles (assuming azimuthal symmetry) yielded beam currents that were higher than the measured beam current by as much as 15%. It is anticipated that these errors were caused by a combination of effects, which included the large probe surface area, charge-exchange ions in the beam, secondary electron emission from both singly- and doubly-charged ions, and a slightly asymmetric beam.

Radial beam current density profiles were taken at five axial locations to determine beam divergence half-angles and thrust losses due to beam divergence. The methods used to determine divergence half-angles and beam divergence thrust losses are discussed in detail in Ref. [10]. Uncertainties in the beam divergence half-angles and thrust losses due to beam divergence cannot presently be assessed due to the unknown sources of error in the beam current density measurements.

Operating Procedures

TAG and NSTAR ion optics were tested on the 30 cm ion thruster at the thruster input power levels and corresponding operating parameters listed in Table 1.

These power levels included NSTAR operating points that encompassed the full 0.5-2.3 kW throttling range,[18] and an operating point with a higher beam voltage for operation up to 3.0 kW. During thruster operation, main and discharge cathode flows were maintained at fixed values while the discharge current was adjusted to maintain a constant beam current.

During each test, the ion optics were initially operated for an extended duration to allow ion optics performance parameters to achieve steady state values. The thruster was operated primarily at TH15 (see Table 1) while monitoring changes in impingement-limited total voltages, electron backstreaming limits, screen grid ion transparencies, and radial beam current density profiles. The thruster was not operated continuously, but was intentionally interrupted on several occasions. When these ion optics performance parameters had achieved steady state values, the thruster was step-ramped through operating points listed in Table 1 to characterize ion optics' performance. At each operating point, ion optics performance parameters such as impingement-limited total voltages, electron backstreaming limits, screen grid ion transparencies, and beam current density profiles, as well as other thruster performance parameters, were determined. Upon completion of each ion optics' performance data sets, the ion optics were re-characterized at TH15 to confirm that ion optics' performance had not changed.

Results and Discussions

Ion Optics Burn-in

The results of ion optics burn-in at TH15 for both ion optics' designs are plotted in Fig. 2. Performance parameters were plotted as a function of propellant throughput and not accumulated operation because the ion optics were operated at several different power levels during this burn-in period. Monitored ion optics performance parameters included perveance margin, electron backstreaming limit, screen grid ion transparency, and beam current density profiles.

TAG Ion Optics

Initial performance tests with TAG ion optics revealed that ion optics performance parameters were indeed changing rapidly with accumulated operation. The thruster was, therefore, operated until these performance parameters achieved steady state values. The thruster was operated at TH15 throughout most of the burn-in period. The thruster was not operated continuously, but was restarted 16 times throughout the burn-in period, and was vented to atmosphere at a propellant throughput of about 240 gm.

All monitored the ion optics performance parameters of Fig. 2 achieved steady state values after processing about 570 gm of xenon. Perveance margins and screen grid ion transparencies increased by about 80 V and 2%, respectively, while the electron backstreaming limit decreased by about 9 V. During this burn-in period, the peak beam current density 49 mm downstream of the optics changed less than about 0.2 mA/cm^2. This change is only about 3% of the total peak beam current density, and is, therefore, considered too small to appreciably affect these performance parameters.

A post-test examination of the TAG ion optics (discussed in a later section) revealed that the accelerator grid aperture diameters had increased by about 4% throughout the perforated diameter and the cold grid gap had also decreased by about 8% at the geometric center of the active area. Using changes in the cold grid gap as an indicator of hot grid gap behavior, it is speculated that the increases in accelerator aperture diameters and grid gap caused the increases in perveance margins and the decreases in electron backstreaming limits because both performance parameters are directly affected by these geometric changes.[13,19] Geometric changes at the ion optics' center are speculated to have contributed significantly to these performance changes because the beam current density is peaked there and, therefore, beamlet currents are largest there. It is further speculated that the cold grid gap decrease at the ion optics' geometric center may have been responsible for the slight increase in screen grid ion transparency. This is because a smaller grid gap is known to reduce discharge losses by improving screen grid ion transparency.[12] TAG ion optics' performance characterization results presented in the remainder of the paper were measured following ion optics burn-in unless otherwise noted.

NSTAR Ion Optics

The results for NSTAR ion optics shown in Fig. 2, and discussed in Ref. [11], showed no significant changes in any of the monitored performance parameters. If a burn-in had occurred for this ion optics set, it would have to have occurred prior to a propellant throughput

of 230 gm. Ion optics' performance characterizations were initiated at 570 gm of propellant throughput. Following performance characterizations, Fig. 2 shows that although perveance margins and electron backstreaming limit remained unchanged, the screen grid ion transparency had decreased by 0.8% for unknown reasons.

Burn-in has been noted with molybdenum ion optics during an NSTAR thruster long duration test.[4] Rapid decreases in perveance margins, screen grid ion transparencies, and electron backstreaming limit magnitudes were noted within the first 150 hours, or 1.3 kg of xenon, of life testing. These changes are consistent with an increasing grid hot gap.

Impingement-Limited Total Voltage

Beam current as a function of impingement-limited total voltage is plotted in Fig. 3 for the TAG and NSTAR ion optics. Perveance margins for the TAG ion optics are listed in Table 2 with results from NSTAR ion optics for comparison.

As Fig. 3 and Table 2 demonstrate, impingement-limited total voltages for the TAG ion optics were only 0-15 V higher than those of the NSTAR ion optics. This close agreement is not surprising, however, since prior studies had shown that the thicker accelerator grid of the TAG ion optics design has relatively little effect on the impingement-limited total voltage.[12,20] Although the accelerator aperture diameters varied significantly for the TAG ion optics, they were similar to the NSTAR ion optics at the active area center, where beam current densities and, therefore, beam currents per hole were highest.

Electron Backstreaming Limit

Electron backstreaming limit voltages for the TAG ion optics are listed in Table 2 with results with NSTAR ion optics for comparison. Since the electron backstreaming limit is also a function of the peak beam current density,[10] the electron backstreaming limit is plotted as a function of the peak beam current density in Fig. 4 for a more appropriate comparison. The data for each grid set are presented at separate beam voltages because the electron backstreaming limit is also a function of beam voltage.[19]

Table 9 shows that electron backstreaming limits for the TAG ion optics were 3-9 V higher than those of the NSTAR optics. Fig. 4 also shows that the electron backstreaming limit as a function of peak beam current density for the TAG ion optics was about 5-11 V higher than that of the NSTAR ion optics at a beam power supply voltage of 1100 V. The higher electron backstreaming limits for TAG ion optics were not only expected due to the increased accelerator grid thickness,[19] but had also been demonstrated for this accelerator grid thickness using a mercury ion thruster.[13]

Screen Grid Ion Transparency

Table 3 lists screen grid ion transparencies for TAG ion optics with results from NSTAR ion optics for comparison. Screen grid ion transparencies for the TAG ion optics were only about 2% lower than those for the NSTAR optics, reflecting the lower physical screen grid open area fraction of the TAG optics from smaller screen grid aperture diameters. It is noteworthy that although screen grid ion transparencies for the TAG ion optics were lower than those for the NSTAR ion optics, discharge losses were still 0-2% lower than those for the NSTAR ion optics, as shown in Table 3. It is speculated that this was largely due to reduced neutral loss rates for the TAG ion optics due to the lower accelerator grid open area fraction, especially at the active area outer perimeter.

Accelerator Current

Table 3 lists accelerator currents for TAG ion optics with results from NSTAR ion optics for comparison. Accelerator currents for the TAG ion optics were 19-43% greater than those for the NSTAR ion optics. This was due, in part, to a sudden increase in accelerator current during TAG ion optics' performance tests. This is demonstrated in Fig. 5 where accelerator current in plotted as a function of propellant throughput during burn-in and performance testing at TH15. Here, the accelerator current increased from 7.5-8.7 mA to just over 10 mA with no change in facility pressure (also shown in Fig. 5). The cause of this sudden change is presently unknown, however, past NSTAR thruster life tests have exhibited initial accelerator current increases followed by a decrease to steady state values within the first 16 kg of xenon throughput.[4]

Prior to this sudden change, however, accelerator currents were still higher than those for the NSTAR ion optics (shown in Fig. 5 prior to performance characterizations). It is speculated that these

differences were largely due to the lower-than-nominal accelerator aperture diameters.

A one-to-one comparison of accelerator currents for TAG ion optics versus NSTAR ion optics is critical for properly assessing the total impulse improvement of TAG ion optics. This is because the accelerator grid erosion rate is directly proportional to the impingement current.[9] TAG ion optics service life assessments to date have assumed accelerator currents equal to those of the NSTAR ion optics. The varying accelerator currents of this TAG ion optics set have made one-to-one comparisons difficult. Proper comparisons of accelerator currents may require long duration testing since prior tests have demonstrated that up to 1500 hours of wear testing may be required for NSTAR ion optics accelerator currents to reach steady state values.[3,4]

Beam Current Density Profiles, Beam Divergence, and Thrust Loss

Peak beam current densities were determined from radial beam current density profiles taken 48-49 mm downstream of the grid center. Sample radial beam current density distributions at THe19 and TH0 are shown in Fig. 6 for both ion optics sets. Radial beam current density distributions at several axial locations are shown in Fig. 7 for TAG ion optics. Table 3 lists peak beam current densities for the TAG ion optics with results from NSTAR ion optics for comparison. As Table 3 shows, peak beam current densities for the TAG ion optics were up to 5% higher than those for NSTAR ion optics. It is speculated that the larger peak beam current densities for the TAG ion optics was due to the smaller screen grid aperture diameters at the perimeter of the active area. This reduced the physical open area fraction in this region, requiring a higher discharge plasma density to provide the required beam current. This caused more ion current to be extracted through the center of the active area.

Figures 6 and 7 also show that beam current density profiles were slightly non-axisymmetric near the active area center for both ion optics' designs. This slight asymmetry occurred at all power levels tested and is an artifact of the thruster discharge chamber plasma.[10]

Beam divergence angles that enclosed 95% of the total beam current are listed in Table 4 for TAG ion optics with results from NSTAR ion optics for comparison. Divergence half-angle data for the TAG ion optics were within 2º of those for the NSTAR ion optics. Sample plots of percentage of total beam current that enclosed a given divergence half-angle are shown in Fig. 8 for TAG and NSTAR ion optics. Beam divergence half-angles were similar for both ion optics' designs.

Table 4 lists these thrust correction factors due to beam divergence for TAG ion optics with results from NSTAR ion optics for comparison. All values for titanium ion optics were within 1% of those with molybdenum ion optics. This close agreement demonstrates that thrust losses from beam divergence are similar for TAG and NSTAR ion optics.

Post-test TAG Ion Optics Examination

Following performance tests, the TAG ion optics were removed and re-inspected. Measured post-test dimensions included accelerator grid aperture diameters and the cold grid gap. Accelerator aperture diameters increased by about 4% throughout the active area, likely due to sputter erosion. The increase in aperture diameter is initially rapid because the aperture wall cusp height can be sputter eroded quickly. The aperture wall cusps are an artifact of the grid fabrication technique. The cold grid gap decreased by about 8% at the geometric center of the ion optics, however, this change was within the accuracy of the measurement.

Pre- and post-test photomicrographs of screen and accelerator apertures were compared. Notches in the accelerator aperture wall cusps were found at and near the apertures of the active area outer perimeter. Pre- and post-test examples are shown in Fig. 9. These notches occurred in apertures as far as 17 mm from the outer-radius and occurred throughout the circumference. The notches are speculated to have been primarily due to the 22% smaller-than-nominal accelerator aperture diameters in this region.

Notching likely occurred during perveance measurements, where reducing the total voltage between the grids defocused ion beamlets, which then impinged directly upon the accelerator aperture wall cusps. The notched appearance is likely due to non-circular beamlets, which are caused by interactions with adjacent beamlets. Beamlet distortion (i.e. non-circularity) would be expected to increase towards the smaller beamlet currents of the outer-perimeter

apertures because beamlet distortion increases with decreasing normalized perveance per hole.[21] Notches only appeared on the portions of the aperture wall cusps that were radially opposite to the geometric center of the grid due to the slight misalignment of the screen and accelerator apertures.

Conclusions

The results of performance tests with TAG ion optics were presented. TAG ion optics utilize a 50% thicker accelerator grid to double ion optics' service life. NSTAR ion optics were also tested to provide a baseline performance for comparison. Both sets were initially operated until ion optics performance parameters achieved steady state values. Afterwards, performance characterizations were conducted. All tests were conducted on the same 30 cm ion thruster that was nearly identical in mechanical design to that of the NSTAR thruster.

All performance parameters for the TAG ion optics achieved steady state values after processing 570 gm of propellant. During this ion optics burn-in, perveance margins and screen grid transparencies increased while electron backstreaming limits decreased. Accelerator aperture diameter increases and cold grid gap decreases were speculated to have caused these changes.

Impingement-limited total voltages for the TAG ion optics were only 0-15 V higher than those of the NSTAR ion optics. This close agreement is not surprising, however, since prior studies had shown that the thicker accelerator grid of the TAG ion optics design has relatively little effect on the impingement-limited total voltage.

Electron backstreaming limits for the TAG ion optics were 3-9 V higher than those for the NSTAR optics. The higher electron backstreaming limits for the TAG ion optics were expected due to the increased accelerator grid thickness.

Screen grid ion transparencies for the TAG ion optics were only about 2% lower than those for the NSTAR optics, reflecting the lower physical screen grid open area fraction of the TAG ion optics from smaller screen grid aperture diameters.

Accelerator currents for the TAG ion optics were 19-43% greater than those for the NSTAR ion optics. This was due, in part, to a sudden increase in accelerator current during TAG ion optics' performance tests. The cause of this sudden change is presently unknown, however, past NSTAR thruster life tests have exhibited initial accelerator current increases followed by a decrease to steady state values. Prior to this sudden change, however, accelerator currents were still higher than those for the NSTAR ion optics. It is speculated that these differences were largely due to the lower-than-nominal accelerator aperture diameters.

Beam divergence half-angles that enclosed 95% of the total beam current for the TAG ion optics were within 2º of those for the NSTAR ion optics. All beam divergence thrust correction factors for the TAG ion optics were within 1% of those with NSTAR ion optics.

A post-test examination of the TAG ion optics revealed that accelerator aperture diameters had increased by about 4% throughout the active area and the cold grid gap had decreased by about 8% at the geometric center of the ion optics. Photomicrographs of TAG accelerator grid apertures showed notching of the accelerator aperture wall cusps located at and near the outer-radius apertures. It is speculated that this notching was created during perveance measurements and was the result of the smaller-than-nominal aperture diameters in this region and the slight under-compensation of the aperture patterns.

References

[1] Rawlin, V.K., et al. "An Ion Propulsion System for NASA's Deep Space Missions," AIAA Paper 99-4612, September 1999.

[2] Polk, J.E., et al., "In-Flight Performance of the NSTAR Ion Propulsion System on the Deep Space One Mission," IEEE Aerospace Conference Paper 8.0304, March 2000.

[3] Polk, J.E., et al., "An Overview of the Results from an 8200 Hour Wear Test of the NSTAR Ion Thruster," AIAA Paper 99-2446, June 1999.

[4] Anderson, J.R., et al., "Performance Characteristics of the NSTAR Ion Thruster During an On-going Long Duration Ground Test," IEEE Aerospace Conference Paper 8.0303, March 2000.

[5] Personal Communication, Anderson, J.R., Jet Propulsion Laboratory, Pasadena, CA, May 2001.
[6] Brophy, J.R., Polk, J.E., and Rawlin, V.K., "Ion Engine Service Life Validation by Analysis and Testing," AIAA Paper 96-2715, July 1996.
[7] Rawlin, V.K., "Erosion Characteristics of Two-Grid Ion Accelerating Systems," IEPC Paper 93-175, September 1993.
[8] Patterson, M.J., et al., "Ion Propulsion Development Activities at NASA Glenn Research Center," AIAA Paper 2000-3810, July 2000.
[9] Soulas, G.C., "Grid Technology Analyses for CNSR," Presentation at NASA Glenn Research Center, January 2000.
[10] Soulas, G.C., Foster, J.E., and Patterson, M.J. "Performance of Titanium Optics on a NASA 30 cm Ion Thruster," AIAA Paper 00-3814, July 2000.
[11] Soulas, G.C., "Performance Evaluation of Titanium Ion Optics for the NASA 30 cm Ion Thruster," IEPC Paper 01-92, October 2001.
[12] Rawlin, V.K., "Performance of 30-cm Ion Thrusters with Dished Accelerator Grids," AIAA Paper 73-1053, October-November 1973.
[13] Rawlin, V.K., "Studies of Dished Accelerator Grids for 30-cm Ion Thrusters," AIAA Paper 73-1086, October-November 1973.
[14] Christensen, J.A., et al., "Design and Fabrication of a Flight Model 2.3 kW Ion Thruster for the Deep Space 1 Mission," AIAA Paper 98-3327, July 1998.
[15] Sovey, J.S., et al., "Development of an Ion Thruster and Power Processor for New Millenium's Deep Space 1 Mission," AIAA Paper 97-2778, December 1997.
[16] Pinero, L.R., Patterson, M.J., and Satterwhite, V.E., "Power Console Development for NASA's Electric Propulsion Outreach Program," IEPC Paper 93-250, September 1993.
[17] Foster, J.E., Soulas, G.C., and Patterson, M.J., "Plume and Discharge Plasma Measurements of a 5 kW NSTAR-Derivative Ion Thruster," AIAA Paper 2000-3812, July 2000.
[18] Rawlin, V.K., et al., "NSTAR Flight Thruster Qualification Testing," AIAA Paper 98-3936, July 1998.
[19] Kaufman, H.R., "Technology of Electron Bombardment Ion Thrusters," Advances in Electronics and Electron Physics, vol. 36, Academic Press, Inc., New York, 1974, pp. 265-373.
[20] Rovang, D.C. and Wilbur, P.J., "Ion Extraction Capabilities of Two-Grid Accelerator Systems," IEPC Paper 84-86, July 1984.
[21] Hayakawa, Y. and Kitamura, S., "Ion Beamlet Divergence Characteristics of Two-Grid Multiple-Hole Ion Accelerator Systems," AIAA Paper 97-33195, July 1997.

Table 1. Nominal thruster operating parameters.

Power Level Designation	Input Power,[a] kW	Beam Current,[b] A	Beam Voltage,[b] V	Accelerator Voltage, V	Neutralizer Keeper Current, A	Main Flow, sccm	Discharge Cathode Flow, sccm	Neutralizer Flow, sccm
TH0[c]	0.5	0.51	650	-150	2.0	5.98	2.47	2.40
TH4[c]	1.0	0.71	1100	-150	2.0	8.30	2.47	2.40
TH8[c]	1.4	1.10	1100	-180	1.5	14.4	2.47	2.40
TH10[c]	1.7	1.30	1100	-180	1.5	17.2	2.56	2.49
TH12[c]	1.8	1.49	1100	-180	1.5	18.5	2.72	2.65
TH15[c]	2.3	1.76	1100	-180	1.5	23.4	3.70	3.60
THe19	3.0	1.76	1500	-250	1.5	23.1	3.54	3.60

[a]Nominal values.
[b]Power supply current or voltage.
[c]Nominal NSTAR operating condition.

Table 2. Perveance margins and electron backstreaming limits for TAG and NSTAR ion optics.

Power Level Designation	Perveance Margin, V		Electron Backstreaming Limit, V	
	TAG	NSTAR	TAG	NSTAR
TH0[a]	175	175	-65	-69
TH4[a]	535	540	-121	-126
TH8[a]	450	455	-132	-138
TH10[a]	405	405	-136	-143
TH12[a]	350	365	-140	-148
TH15[a]	285	295	-147	-156
THe19	755	760	-194	-197

[a]Nominal NSTAR operating condition.

Table 3. Peak beam current densities, screen grid ion transparencies, discharge losses, and accelerator currents for TAG and NSTAR ion optics.

Power Level Designation	Peak Beam Current Densities,[a] mA/cm^2		Screen Grid Ion Transparencies		Discharge Losses,[b] W/A		Accelerator Currents, mA	
	TAG	NSTAR	TAG	NSTAR	TAG	NSTAR	TAG	NSTAR
TH0[b]	2.4	2.4	0.820	0.836	250	250	2.0	1.4
TH4[b]	3.3	3.2	0.868	0.882	240	240	2.2	1.8
TH8[b]	4.5	4.3	0.872	0.877	200	200	5.0	3.5
TH10[b]	5.0	4.8	0.864	0.870	190	191	6.3	4.5
TH12[b]	5.5	5.3	0.856	0.863	185	187	7.8	5.5
TH15[b]	6.1	5.8	0.839	0.849	184	188	10.1	7.2
THe19	6.3	6.0	0.892	0.895	176	178	8.1	6.8

[a]Peak beam current densities at 48-49 mm downstream of the geometric center of the ion optics; peak beam current densities occurred at approximately the radial center of the grid active area.
[b]Nominal NSTAR operating condition.

Table 4. Divergence half-angles that enclosed 95% of total beam current and beam divergence thrust correction factors for TAG and NSTAR ion optics.

Power Level Designation	Divergence Half-angle at 95% of Beam Current, degrees		Thrust Correction Factor for Beam Divergence	
	TAG[a]	NSTAR	TAG[a]	NSTAR
TH0[b]	28	29	0.97	0.97
TH4[b]	-	29	-	0.97
TH8[b]	29	29	0.97	0.97
TH10[b]	-	28	-	0.97
TH12[b]	-	27	-	0.98
TH15[b]	25	26	0.98	0.98
THe19	31	29	0.97	0.97

[a]Determined with data taken prior to ion optics burn-in.
[b]Nominal NSTAR operating condition.

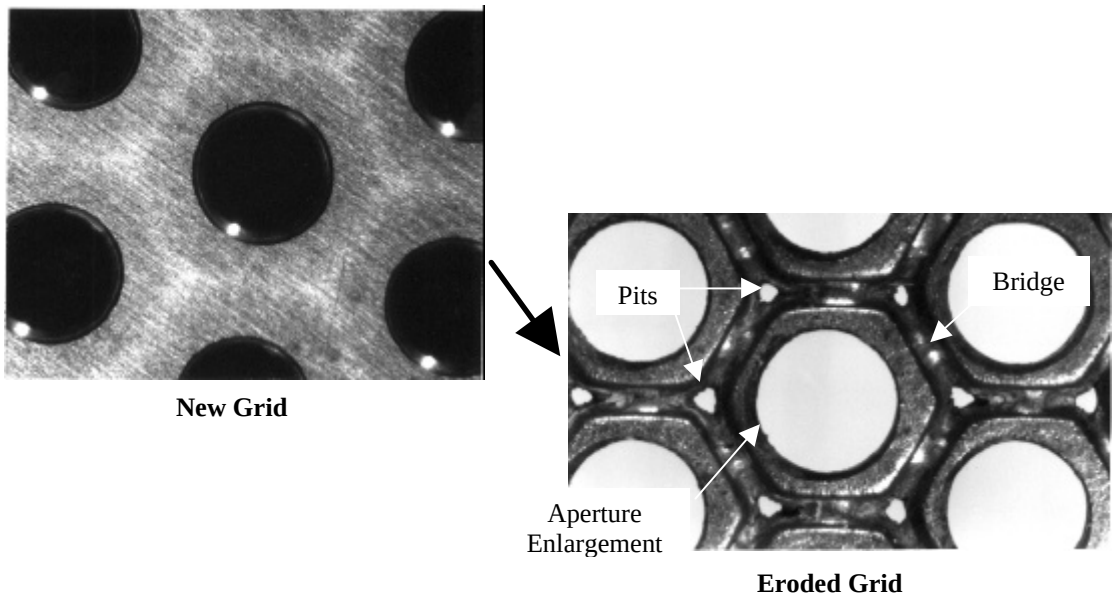

Fig. 1. Typical accelerator grid erosion sites.

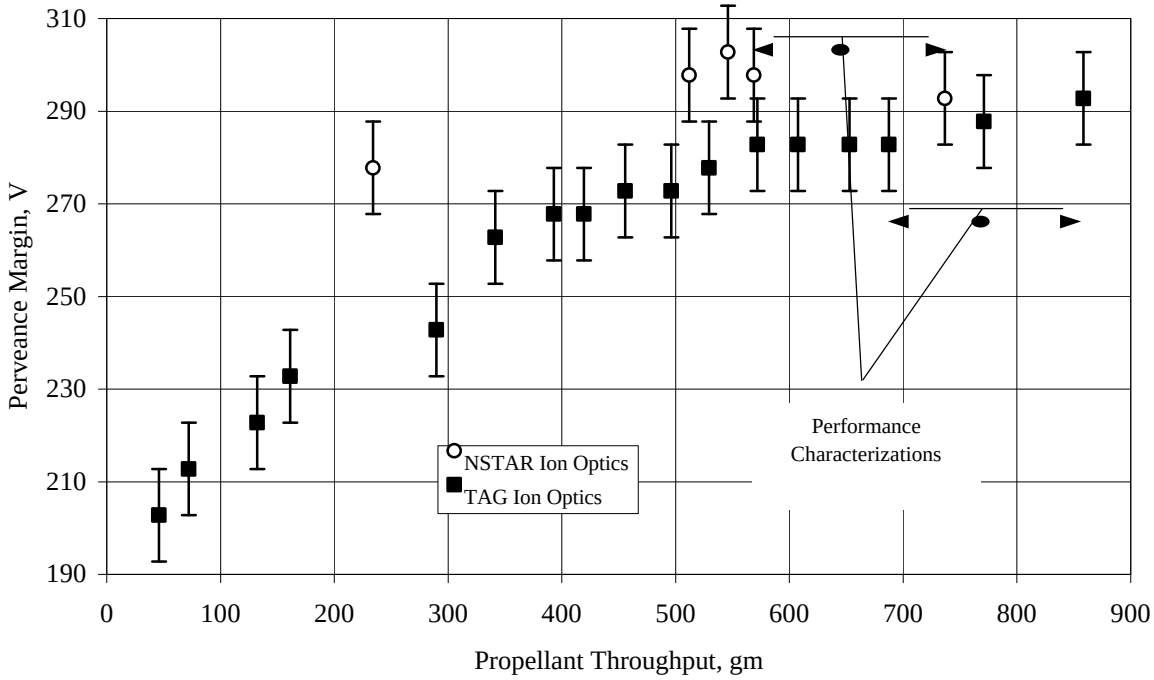

a. Perveance margin as a function of accumulated propellant throughput.

Fig. 2. Burn-in performance parameters at TH15 for TAG and NSTAR ion optics. (Continued)

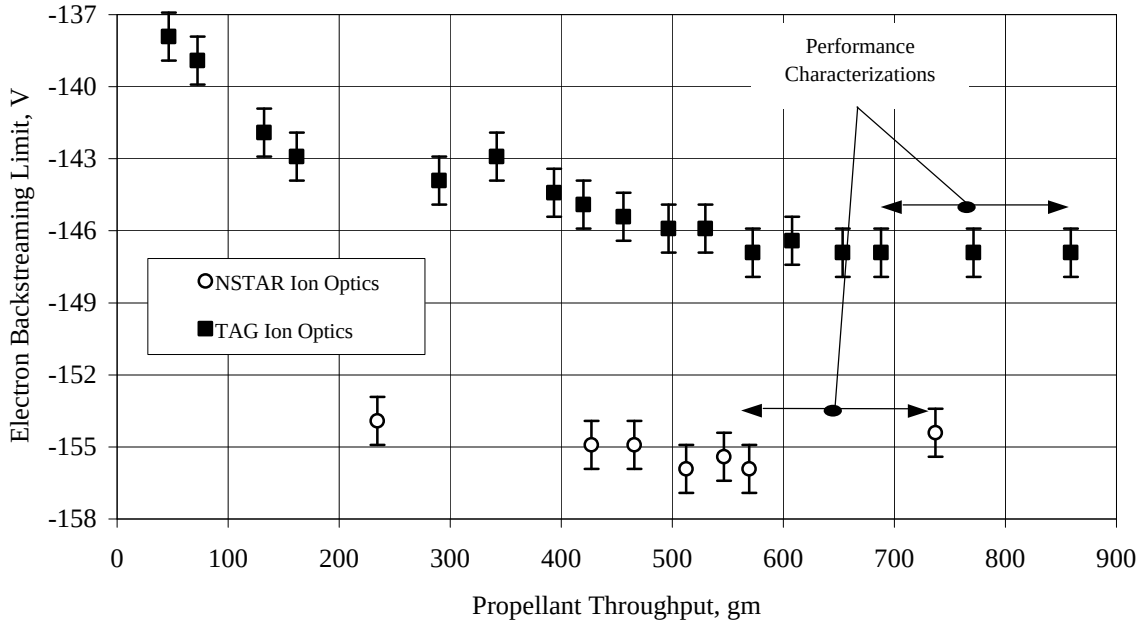

b. Electron backstreaming limit as a function of accumulated propellant throughput.

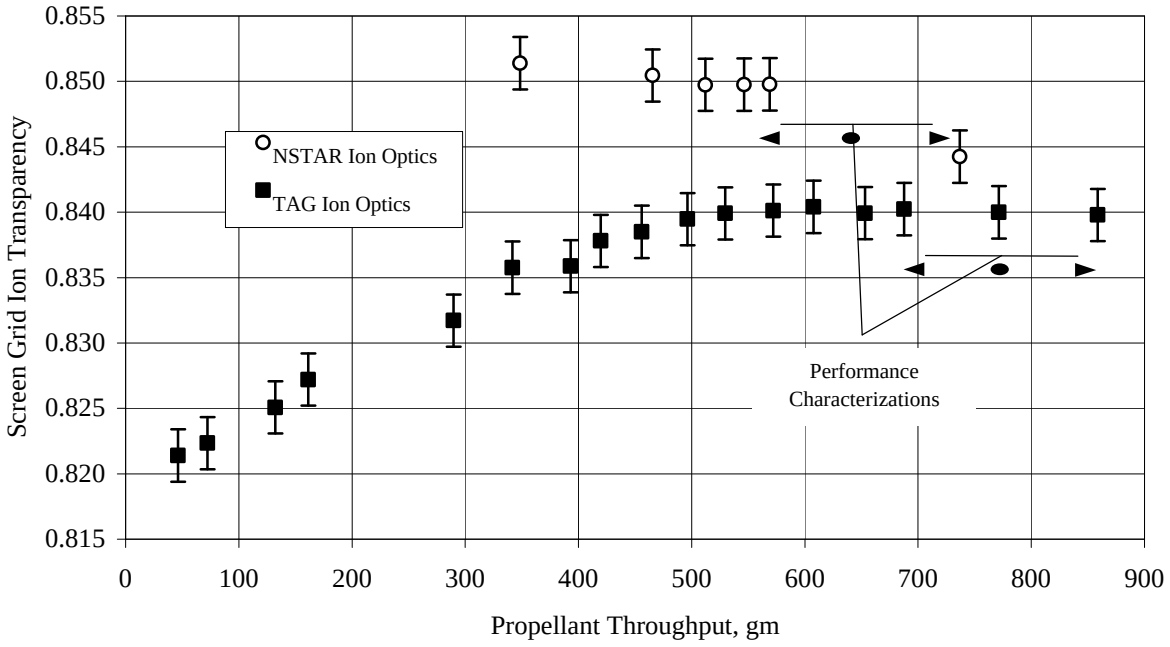

c. Screen grid ion transparency as a function of accumulated propellant throughput.

Fig. 2. Burn-in performance parameters at TH15 for TAG and NSTAR ion optics. (Concluded)

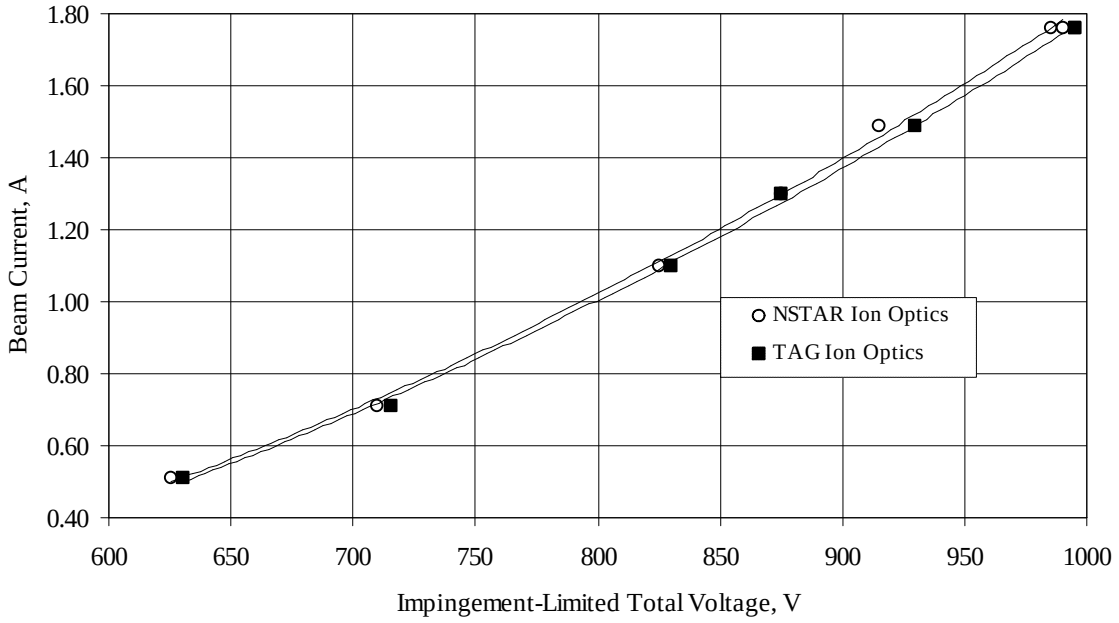

Fig. 3. Beam current as a function of impingement-limited total voltage for TAG and NSTAR ion optics.

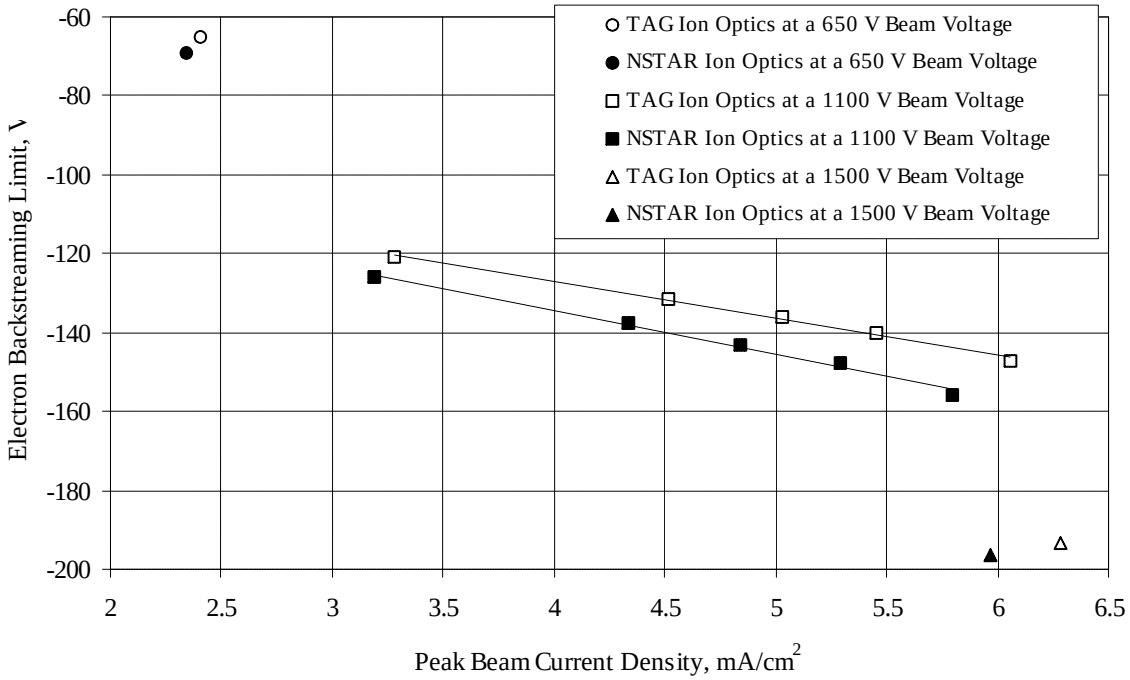

Fig. 4. Electron backstreaming limit as a function of peak beam current density for TAG and NSTAR ion optics. Peak beam current densities were measured 48 mm downstream of the ion optics' center. Beam voltages here are power supply voltages.

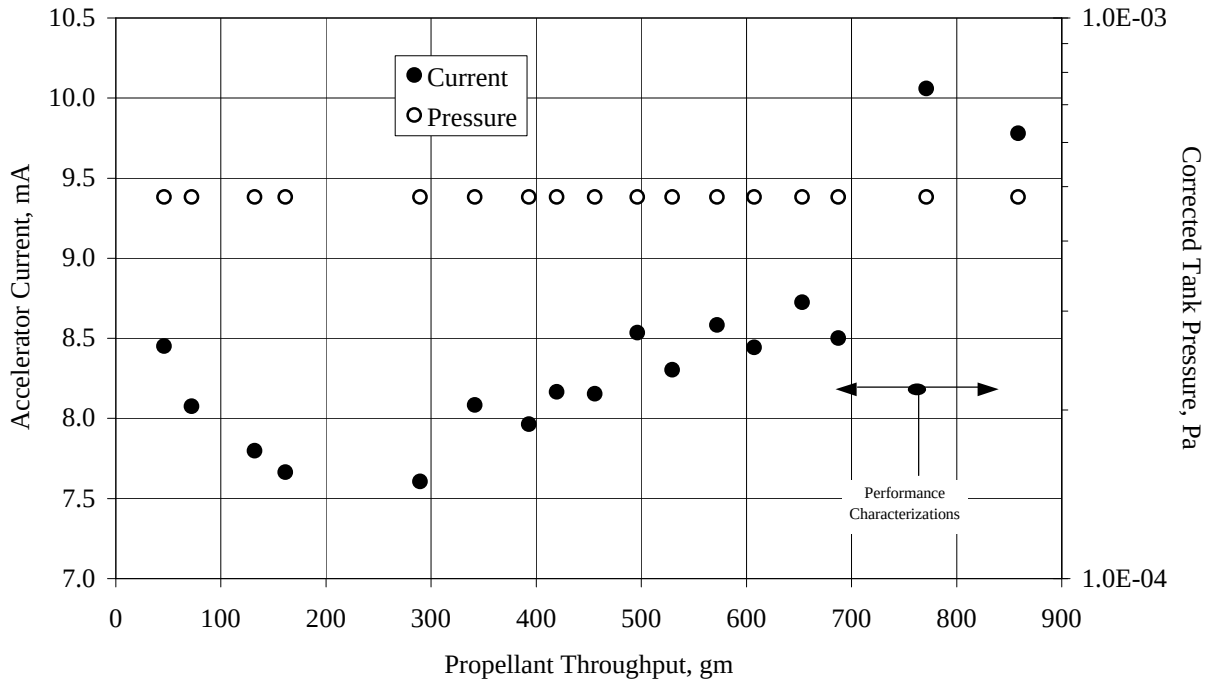

Fig. 5. Accelerator current and corrected tank pressure as a function of propellant throughput for TAG ion optics at TH15.

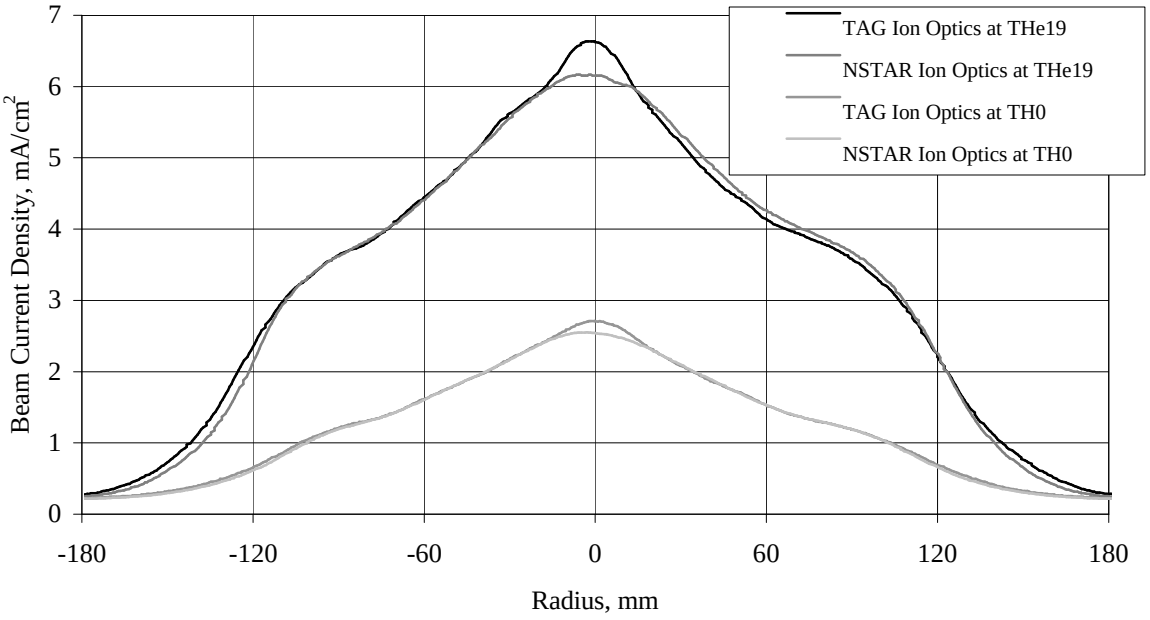

Fig. 6. Radial beam current density profiles for TAG and NSTAR ion optics at THe19 and TH0. Beam current densities were measured 48-49 mm downstream of the ion optics' center. Beam current densities for TAG ion optics were measured prior to ion optics burn-in.

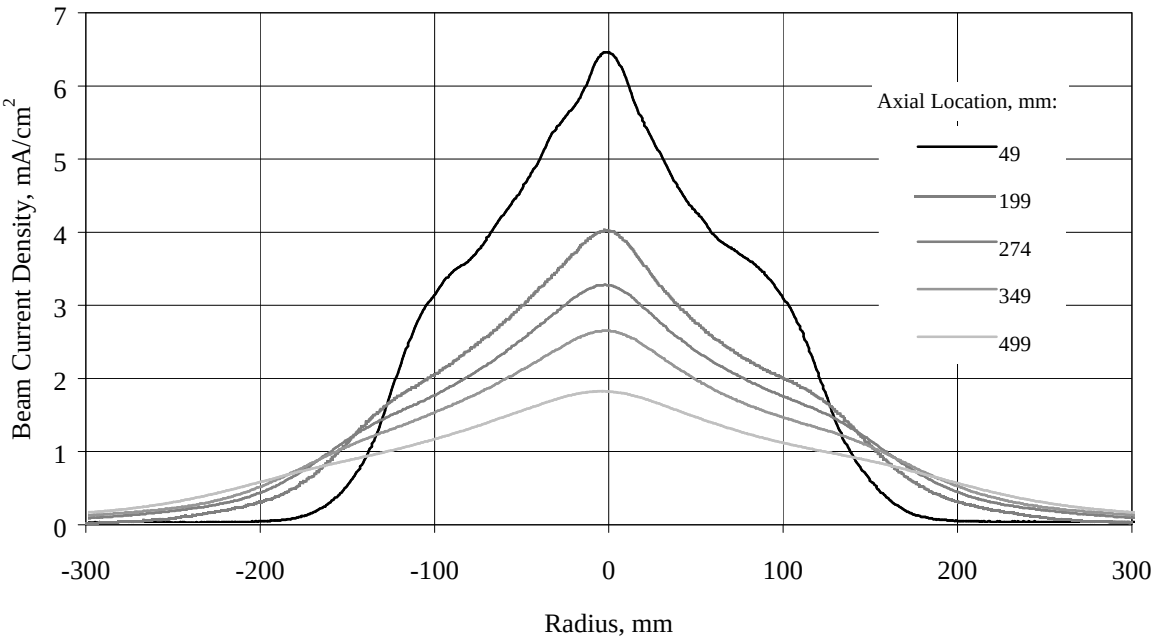

Fig. 7. Radial beam current density profiles at several axial locations for TAG ion optics at THe19. Beam current densities for TAG ion optics were measured prior to ion optics burn-in.

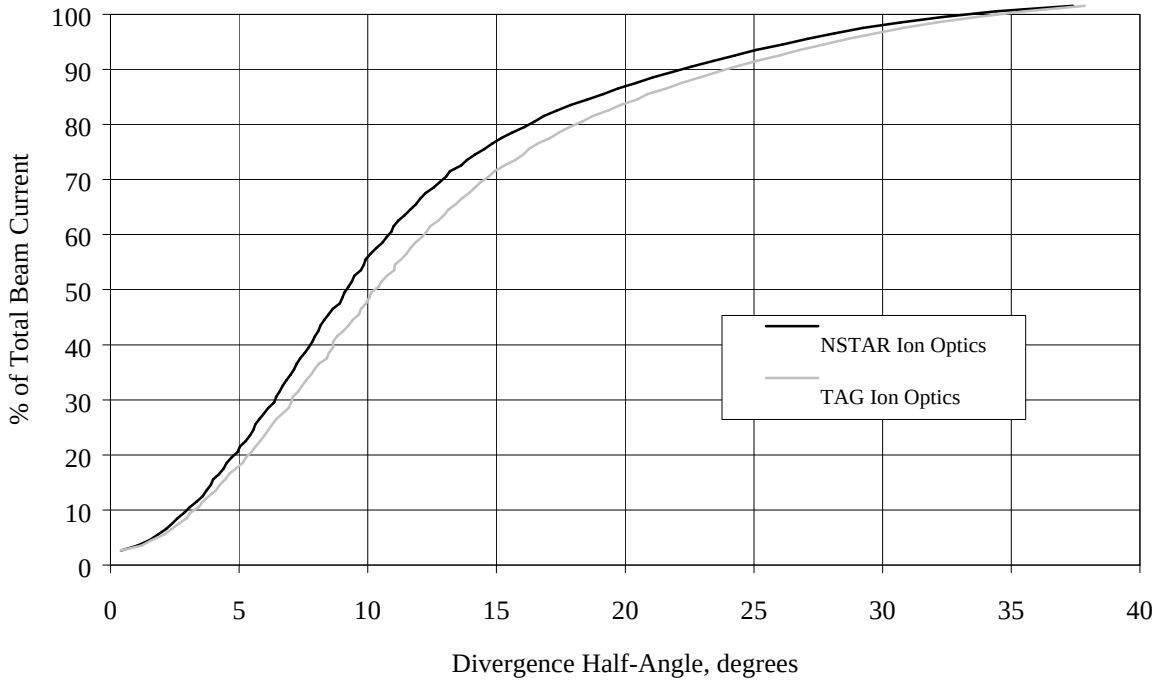

Fig. 8. Percentage of total beam current enclosed in a given divergence half-angle for TAG and NSTAR ion optics at a THe19. Beam current densities for TAG ion optics were measured prior to ion optics burn-in.

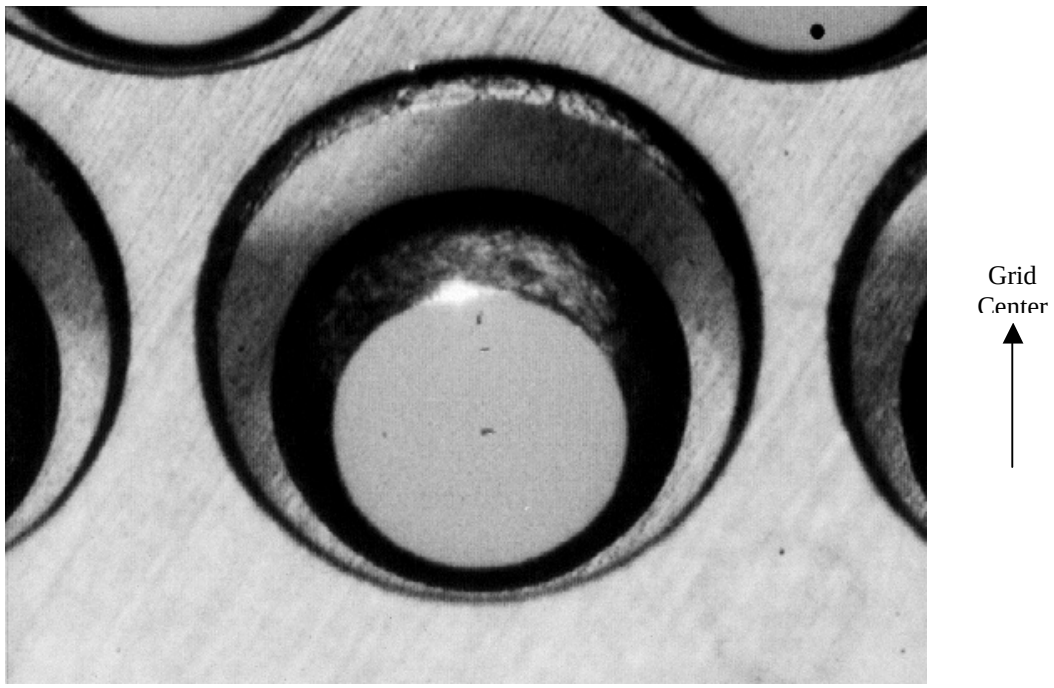

a. Pre-test photomicrograph.

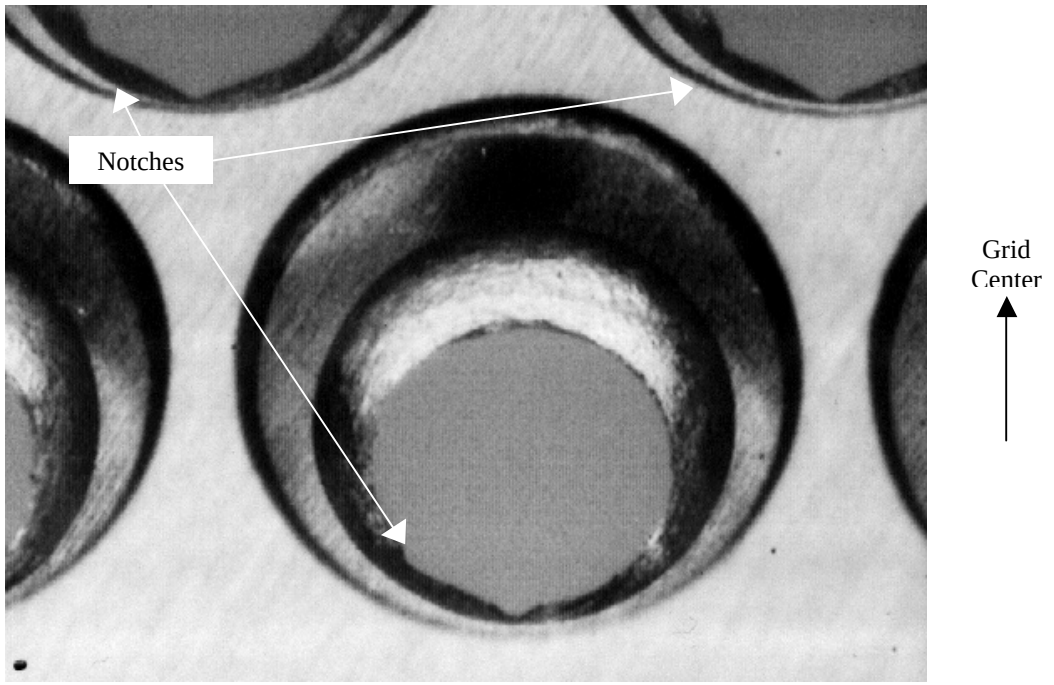

b. Post-test photomicrograph.

Fig. 9. Pre- and post-test photomicrographs of TAG ion optics' screen and accelerator apertures at the outer-radius of the active area.